A PREDICTION MODEL OF THERMAL CONDUCTIVITY
OF ROCK USING MEASUREMENTS IN BIPHASIC MIXTURES

Ariston de Lima Cardoso[1], Roberto Max de Argollo[2] and Alexandre Barreto Costa[3]

ABSTRACT. In this study, we developed a model to predict the thermal conductivity of full rocks from measurements on biphasic mixtures of grains of these rocks. Firstly, we measured the density and thermal conductivity of the full rock samples. The full samples were then grounded and we measured the effective thermal conductivity of mixtures prepared with grains of these rocks in different porosities using air as saturating. Using the flexible model of thermal conduction developed in this study, which we call Geoterm, and the rule of generalized mixture due to Korvin, we calculated the average values of the numerical factors of the equations of these two models and, with these equations, we predicted the thermal conductivity of the integrity rock by adjusting the equations of these models with experimental data. Even with these equations and the data of the integrity rocks and mixtures, we predicted the effective thermal conductivity of the samples for the various porosities of the mixtures. The predicted results for the full rock, as compared to the measured values, showed small and large discrepancies due to the large variation range of the thermal conductivity of the full rocks, resulting in ranges also wide for the numerical factors of the two equations. In agreement with Krupiczka empirical expression, the values predicted by the Geoterm and Korvin models for effective thermal conductivity showed lower discrepancies when compared to other models observed in this study.

Keywords: rock thermal conductivity, effective thermal conductivity, binary mixture model.

RESUMO. Neste estudo, desenvolvemos um modelo para predizer a condutividade térmica de rochas íntegras a partir de medidas em misturas binárias de grãos destas rochas. Primeiramente, medimos a densidade e a condutividade térmica das amostras das rochas íntegras. As amostras foram, em seguida, moídas e medimos a condutividade térmica efetiva de misturas preparadas com os grãos dessas rochas em diferentes porosidades usando ar como saturante. Usando o modelo flexível de condução térmica desenvolvido neste estudo, denominado Geoterm, e a regra da mistura generalizada de Korvin, calculamos os valores médios dos fatores numéricos das equações destes dois modelos e, com estas predissemos a condutividade térmica da rocha íntegra pelo ajuste dos parâmetros desses modelos com os dados experimentais. Ainda com essas equações e com os dados das rochas íntegras, como também das misturas, predissemos a condutividade térmica efetiva das amostras para as várias porosidades das misturas. Os resultados preditos para a amostra íntegra, quando comparados aos valores medidos, apresentaram discrepâncias pequenas e grandes, consequência de a faixa de variação da condutividade térmica das rochas ser bem larga resultando em faixas também largas para os fatores numéricos das duas equações. Em concordância com a expressão empírica de Krupiczka, os valores preditos pelos modelos Geoterm e Korvin para condutividade térmica efetiva mostraram menores discrepâncias quando comparados a outros modelos verificados neste estudo.

Palavras-chave: condutividade térmica de rocha, condutividade térmica efetiva, modelo de mistura binária.

[1]Universidade Federal do Recôncavo da Bahia, Centro de Ciências Exatas e Tecnologia, Campus de Santo Antônio de Jesus, BA, Brazil. Phone: +55(71) 9944-4425 – E-mail: ariston@ufrb.edu.br

[2]Universidade Federal da Bahia, Instituto de Física, Departamento de Física da Terra e do Meio Ambiente, Rua Barão de Jeremoabo, 40170-115 Salvador, BA, Brazil. Phone: +55(71) 3283-6680; Fax: +55(71) 3283-6681 – E-mail: robmax@ufba.br

[3]Universidade Federal da Bahia, Instituto de Física, Departamento de Física da Terra e do Meio Ambiente, Rua Barão de Jeremoabo, 40170-115 Salvador, BA, Brazil. Phone: +55(71) 3283-6694; Fax: +55(71) 3283-6681 – E-mail: abc@ufba.br

INTRODUCTION

Knowledge of the thermal properties of rocks is important in quantitative studies of sedimentary basin evolution to construct models that describe the thermal history of the basin. The thermal conductivity of rocks is commonly measured in solid samples with dimensions that are compatible with the measuring instrument. However, it is often necessary to make these measurements using fragmented rock samples. In the oil industry, for example, coring wells is expensive, and the thermal conductivity of sedimentary and crystalline rock samples must be determined using drill cuttings. To do so, mixtures of the ground samples are prepared, and models are used to obtain the thermal conductivity from measurements of the effective thermal conductivity (ETC) of the mixtures. The conductivity of the rock grains depends on several factors, such as the mineralogical composition, texture, structure, type and amount of fluid saturation, density, anisotropy and porosity. These parameters and properties, which are closely related to the formation processes of the minerals and rocks, make the determination of the thermal properties of fragmented samples a complex task that requires theoretical or empirical modeling.

Petrophysical studies often require ETC measurements of binary mixtures of rock grains that are saturated by air. Several models and formulations have been proposed to predict such measurements; all of them combine the porosity of the mixture and the thermal conductivity of the mixed phases, and some include an empirical factor. However, the appropriate model for a given mixture is not always clear. Of the models available in the literature, some have been applied to sedimentary rocks (e.g., Anand et al., 1973; Tenchov, 1998), while others have been applied to sands (e.g., Tavman, 1996). We are not aware of models that have been applied to igneous and metamorphic rocks.

In this paper, we develop a model to predict thermal conductivity of full rocks from measurements on binary mixtures of grains of these rocks. Firstly, we made measurements in the whole samples; then, the samples were ground and prepared mixtures with the grains. The samples were collected from outcrops of basement rocks on the northeast Brazilian coast. The lithologies analyzed in this work include granite, gneiss, ortho-derived rocks and metasandstone.

This work is part by the Geoterm-Ne project, under which the samples were collected, funded by Petrobras-Cenpes-Promob and by the National Institute of Science and Technology of Petroleum Geophysics – INCT-GP.

Thermal Measurements and Effective Thermal Conductivity Models

Thermal conductivity measurements are usually made by studying the transient behavior of a heat pulse that is injected into the material. In granular materials, the irregularities, heterogeneity and roughness of the grains complicate the heat transfer mechanism in the mixture. The heat is transported by conduction in the solid grains and in the fluid, by convection in the fluid and by radiation between the grains. The heat transport by radiation is negligible in mixtures of small grains at temperatures below 200°C; and the convection of heat is negligible in grains with diameters less than 1 cm (Woodside, 1958 apud Woodside & Messmer, 1961). In this study, we neglect the effects of radiation and convection and consider small grains (less than 3 mm) at room temperature.

In conductive transport, the heat pulse propagates through the pores and grains of the mixture, and the driving mechanism of the heat transfer depends on the relationships between the thermal properties of the solid grains and the saturating fluid. For mixtures in which the thermal conductivity of the solid is greater than that of the fluid, most of the heat is conducted through the solid grain contacts. This type of mixture is defined by some authors as external porosity. When the thermal conductivity of the solid is less than that of the fluid, heat flows primarily in the fluid phase, and the porosity is said to be internal (e.g., Carson et al., 2005).

Mixture models can be described by combining the values of the quantity to be determined in the solid samples with the volume fraction of each material in the mixture. In a mixture that contains n elements with the same physical property G_i and volume fraction ϕ_i, Lichtenecker & Rother (1931) apud Tenchov (1998) and Korvin (1982) showed that the physical property of the mixture G can be represented by:

$$G = \left[\sum_l^n \phi_i G_i^t \right]^{l/t} \quad \text{when} \ t \neq 0 \qquad (1a)$$

$$G = \exp \left(\sum_l^n \phi_i \ln G_i \right) \quad \text{when} \ t = 0, \qquad (1b)$$

and

$$\sum_l^n \phi_i = 1, \qquad (1c)$$

where t is a real number called of geometric distribution factor.

From Eq. (1a), in a binary mixture that consists of solid grains with a thermal conductivity λ_s that is uniformly distributed in a host fluid with a thermal conductivity λ_a, the (ETC) λ_{ef} is expressed by

$$\lambda_{ef}\left[\phi\lambda_a^t + (1-\phi)\lambda_s^t\right]^{l/t}. \qquad (2)$$

Korvin (1982) developed the general mixture rule using the theory of functional equations under appropriate boundary conditions and showed that Eq. (2) is exact and represents the only function for a two-phase composite with $t, t \neq 0$, some arbitrary real number in $(-\infty, +\infty)$.

Several models and expressions have been proposed to predict the ETC in binary mixtures as a function of the thermal conductivity of each phase and the porosity. Most of these models are based on a few basic structural models, specifically the series, parallel, geometric, Maxwell (in its many forms) and effective medium theory (EMT) models. In the series (Eq. (3)), parallel (Eq. (4)) and geometric (Eq. (5)) models, the ETC is given by the weighted harmonic, weighted arithmetic and geometric weighted means, respectively, of the two phases of the mixture:

$$\begin{aligned}\lambda_{ef} &= \frac{1}{\phi/\lambda_a + (1-\phi)/\lambda_s} \\ &= \frac{\lambda_a\lambda_s}{(1-\phi)\lambda_a + \phi\lambda_s},\end{aligned} \qquad (3)$$

$$\lambda_{ef} = \phi\lambda_a + (1-\phi)\lambda_s \qquad (4)$$

$$\lambda_{ef} = \lambda_a^\phi\lambda_s^{1-\phi} \qquad (5)$$

Eqs. (3) to (5) can be obtained from the Korvin model (Eq. (2)) with $t = -1$ (series model), $t = 1$ (parallel model) and $t = 0$ (geometric model), respectively; the latter is the limit of Eq. (2) by the L'Hospital rule. In the series and parallel models, the phases in the mixture are arranged in layers that are perpendicular and parallel to the direction of heat flow, respectively, while in the geometric model, the phases are randomly distributed. The series and parallel models therefore define the minimum and maximum limits of the ETC of a mixture in which the volume fractions and the thermal conductivities of the components are accurately known and heat transport is only conductive (Carson et al., 2006).

The Maxwell model (Maxwell, 1954) yields an exact solution for the effective electrical conductivity for small spheres dispersed within a continuous medium when the spheres are far enough apart to not interact with each other. The Maxwell-Eucken (Eucken, 1940 apud Carson et al., 2006; Maxwell, 1954) model is the Maxwell model applied to thermal conductivity; in it, the

spheres are sufficiently far apart that local variations in the temperature around each sphere do not interfere with the temperatures around the neighboring spheres.

In binary mixtures, the Maxwell-Eucken model (ME) is divided into two models: the inferior ME model (ME-I) for external porosity mixtures, in which the solid is the dispersed phase and air is the continuous phase (Eq. (6)):

$$\lambda_{ef} = \lambda_a\frac{3\lambda_s - 2(\lambda_s - \lambda_a)\phi}{3\lambda_a + (\lambda_s - \lambda_a)\phi} \qquad (6)$$

and the superior ME model (ME-S) for internal porosity mixtures, where the solid is the continuous phase (Eq. (7)):

$$\lambda_{ef} = \lambda_s\frac{3\lambda_s + (\lambda_a - \lambda_s)(1 + 2\phi)}{3\lambda_s + (\lambda_a - \lambda_s)(1 - \phi)}. \qquad (7)$$

The EMT model (Landauer, 1952) assumes a completely random distribution for all phases and is described by the sum

$$\sum_i \phi_i\frac{\lambda_i - \lambda_{ef}}{\lambda_i + 2\lambda_{ef}} = 0. \qquad (8)$$

For a binary mixture of solid grains with air as the saturant the EMT model can be expressed by Eq. (9) which lies within the Korvin bounds and the Maxwell-Eucken limits. It is an identifier

$$\begin{aligned}\lambda_{ef} = \frac{1}{4}\big\{&(3\phi - 1)\lambda_a - (3\phi - 2)\lambda_s \\ &+ \sqrt{[(3\phi - 1)\lambda_a - (3\phi - 2)\lambda_s]^2 + 8\lambda_a\lambda_s}\big\}.\end{aligned} \qquad (9)$$

that can be used to characterize a mixture as internal or external porosity; those mixtures that lie between the ME-I and EMT models are external porosity mixtures, and those that lie between the EMT and ME-S models are internal porosity mixtures (Carson et al., 2005).

Figure 1 shows ETC versus porosity graphs for the models described above. The parallel (curve a) and series (curve f) models define boundaries that enclose all of the other models; these curves correspond to the Korvin model for $t = 1$ and $t = -1$, respectively, and thus represent the maximum and minimum bounds of the ETC for a biphasic mixture. Curves (b) and (e) represent models ME-S and ME-I, respectively, which define stricter limits within the Korvin bounds. Internal porosity mixtures plot in the region between curves (b) and (c), and mixtures of external porosity fall between curves (c) and (e). Curve (d) represents the geometric model, which coincides with the Korvin model at $t = 0$.
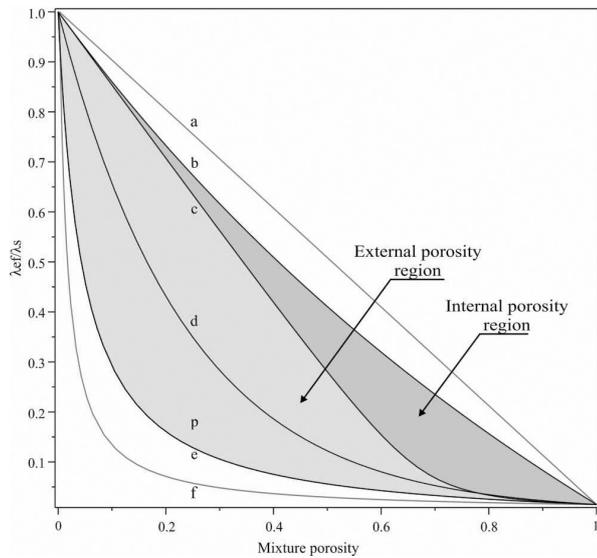
Figure 1 – ETC graphs of the models: (a) parallel; (b) superior Maxwell-Eucken; (c) effective medium theory (EMT); (d) geometric; (e) inferior Maxwell-Eucken; (f) series. Curves (a) and (f) define the Korvin bounds; curves (b) and (e) are the ME limits of the Maxwell-Eucken's model; curves (b) and (c) define the region of internal porosity; and curves (c) and (e) define the region of external porosity. ($\lambda_s/\lambda_a = 100$).

Empirical expressions

Many empirical expressions have been proposed for the ETC of granular binary mixtures. Krupiczka (1967) obtained numerical solutions for the ETC of granular materials for a model consisting of long cylinders and another consisting of spheres in a cubic lattice. He correlated the solutions of these models by taking into account the porosity and derived the equation:

$$\lambda_{ef} = \lambda_f (\lambda_s/\lambda_f)^{A+B \log(\lambda_s/\lambda_f)} \quad (10)$$

with $A = 0.280 - 0.751 \log \phi$ and $B = -0.057A$. Eq. (10) is valid for $0.215 \leq \phi \leq 0.476$.

Woodside & Messmer (1961) constructed a modified resistor model to predict the ETC of porous media by combining series and parallel models and using the electrical conductivity of an aggregate of conductive particles saturated with an electrolytic conductor as an analog. The equation obtained for the ETC in this model is

$$\lambda_{ef} = \frac{a\lambda_f \lambda_s}{\lambda_s(1-d) + d\lambda_f} + c\lambda_f \quad (11)$$

where $c = \phi - 0.03$, $a = (1-c)$ and $d = ((1-\phi)/a)$ and c is taken from Stephenson & Woodside (1958) apud Woodside & Messmer (1961).

Flexible models

Models described by only the thermal conductivities ϕ_i and volume fractions ϕ_i are referred to as rigid models, while those involving an additional parameter are referred to as flexible models. Krischel's model (Krischel, 1963 apud Carson et al., 2006) is the most commonly used flexible ETC model. This model, which is expressed by Eq. (12), combines the series and parallel models with a numerical factor p known as a weighting factor. Krischel's model reduces to the series model for $p = 0$ and to the parallel model for $p = 1$, so the graph of Eq. (12) lies within the entire region between the Korvin bounds when p varies from 0 to 1. Many other flexible models that can cover the Korvin region by choosing different values of the parameter p have been proposed (see Carson et al., 2006). Because these models can be constructed for any experimental points by adjusting the parameter p, they allow for better performance than other models. The problem is choosing a value for the weighting factor p. Several studies have attempted to correlate the factor p with characteristics such as the shape, dimensions and porosity of the grains, but these correlations are dependent on empirical constants; because p is determined empirically, the correlations are not generally valid.

$$\lambda_{ef} = \frac{(1-p)\lambda_f \lambda_s}{(1-\phi)\lambda_f + \phi\lambda_s} + p[\phi\lambda_f + (1-\phi)\lambda_s] \quad (12)$$

METHODOLOGY

The 19 rock samples analyzed in this work, including six granites (Gr), four gneisses (Gn), four orthoderived rocks (Or) and five metasandstones (Me), were collected from basement outcrops along the northeastern Brazil coastline during the project Geoterm-Ne. In these whole rock samples, we analyzed the mass density and the thermal conductivity. The mass density was determined with a water pycnometer developed by Oliveira (2006) which provides measurement precision of 0.2%. The thermal conductivity was measured with a thermal properties analyzer, a Quickline-30, equipped with a planar type sensor covering a range from 0.1 to 6.0 W m⁻¹ K⁻¹ in a laboratory with temperature stabilized in 22°C. Rock samples were kept in the laboratory for at least 48 h before being measured to acquire the same temperature. We made measurements on well polished faces to reduce the effect of thermal contact resistance between the sensor and the rock material. To account for the possible effects of anisotropy, we made measurements on two mutually perpendicular polished faces to obtain average values of the thermal rock conductivity. We made a minimum of three measurements on each face and

take the average value to minimize effects of the heterogeneity of the rock. The precision for the thermal conductivity measurement is 10%.

After these analyses were performed, the whole rock samples were ground to grains with size of medium sand. We prepared binary mixtures of the dried grains in a cylindrical container 60 mm in diameter and 140 mm high using air as saturant. To obtain the porosity, we calculated the volume of the mixture by measuring its mass and using the density determined from the whole sample. The porosity of the mixture was changed by compressing the mixture in the cylinder to ensure a homogeneous density throughout the column. This preparation allows an error of about 3% for the porosity determination.

For each sample, we measured the ETC using the same analyzer equipped with a needle sensor for the range from 0.2 to 1.0 W m^{-1} K^{-1}. The needle is 105 mm long, 0.8 mm in diameter and has a heat source at its midpoint together with a thermistor to monitor the temperature. The needle was introduced into the cylinder through an orifice at its bottom so that it is completely involved by the mixture. For each sample, we measured the thermal conductivity for at least three porosity values to verify the behavior between conductivity and porosity. The measures in the mixtures were made in the laboratory with permanently stabilized temperature, and the precision for the ETC measurements is 10%.

RESULTS AND DISCUSSION

Table 1 presents the specific gravity (ρ) and average thermal conductivity (λ_s) measurements obtained in full rock samples as well as the porosity (ϕ) and the ETC determined in the mixtures. The error in the measurements of density and thermal conductivity are 0.5% and 10% respectively. As described above, we measured the ETC for a minimum of three porosity values of each mixture. The porosities of the samples were between 0.262 and 0.505, and the ETC values ranged from 0.188 to 0.392 W m^{-1} K^{-1}.

In Figure 2, the experimental results from Table 1 are plotted on the ETC graphs from Figure 1. Should be noted that about two-thirds of these points corresponds to measurements of a same sample at different porosities. Figure 2 shows that all of the measurements lie within the Korvin model, which characterizes the mixtures as binary. In addition, the measurements fall between the EMT and ME-I models, which characterizes the mixtures as external porosity one; this indicates that the heat conduction in these mixtures is primarily through the rock grains.

In Figure 2, it is observed that all of the points lie between the curves of the geometric and ME-I models. The orthoderived

and metasandstone rock samples plot across the bottom of the region formed by these two models, while the gneisses plot further to the top and the granite plots in the central region. In general, however, the distribution appears to be independent of lithology.
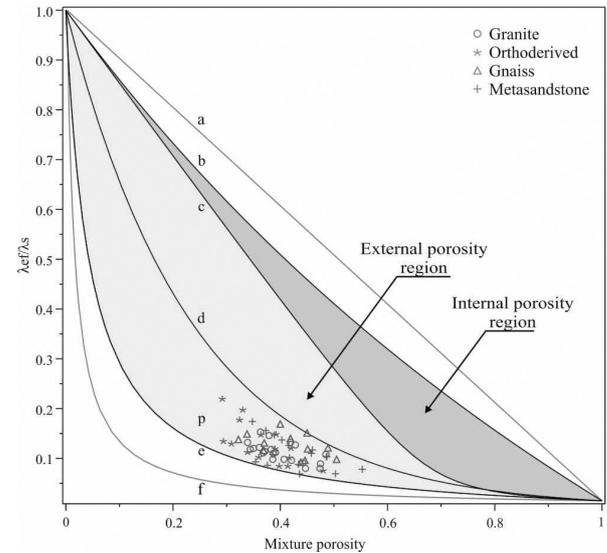

Figure 2 – Data from Table 1 plotted on the ETC graphs from Figure 1. $\lambda_s/\lambda_a = 100$.

The observation that the ETC values measured in the binary mixtures of rock grains from diverse lithologies and with a broad spectrum of thermal conductivity occupy a limited region on the graph led us to build a flexible type thermal conduction model type that is more spatially restricted than the Korvin model in an attempt to achieve more accurate results for the ETC of these mixtures. This new model, which we call Geoterm, is expressed by Eq. (13) and combines the geometric (Eq. (5)) and inferior Maxwell-Eucken (Eq. (6)) models with a weighting factor p: for $p = 0$, Geoterm reduces to the ME-I model, and for $p = 1$, Geoterm reduces to the geometric model. The graph of Eq. (13) lies in the region between the curves of these two models when p varies from 0 to 1.

$$\lambda_{ef} = (1-p)\lambda_f \frac{2\lambda_f + \lambda_s - 2(\lambda_f - \lambda_s)(1-\phi)}{2\lambda_f + \lambda_s + (\lambda_f - \lambda_s)(1-\phi)} + p\lambda_f^{\phi}\lambda_s^{1-\phi}. \qquad (13)$$

These two models were chosen because the points plotted between their curves (see Fig. 2) and because the monotonic behaviors of these curves were similar, particularly in the porosity

Table 1 – Density (ρ, kg m^{-3}) and thermal conductivity (λ_s, W m^{-1} K^{-1}) measurements in whole rock samples and porosity (ϕ) and ETC (λ_{ef}, W m^{-1} K^{-1}) measurements in the mixtures.

Sample	ρ	λ_s	ϕ	λ_{ef}	Sample	ρ	λ_s	ϕ	λ_{ef}
Gr 01	2,588	2.11	0.467	0.228	Gn 10	2,647	2.54	0.338	0.378
Gr 01	2,588	2.11	0.428	0.268	Or 11	2,509	1.75	0.391	0.260
Gr 01	2,588	2.11	0.419	0.278	Or 11	2,509	1.75	0.329	0.346
Gr 01	2,588	2.11	0.379	0.308	Or 11	2,509	1.75	0.291	0.385
Gr 01	2,588	2.11	0.363	0.323	Or 12	2,650	2.01	0.419	0.243
Gr 02	2,663	2.20	0.475	0.195	Or 12	2,650	2.01	0.363	0.298
Gr 02	2,663	2.20	0.383	0.259	Or 12	2,650	2.01	0.323	0.358
Gr 02	2,663	2.20	0.339	0.291	Or 13	2,839	3.35	0.479	0.255
Gr 03	2,638	2.69	0.474	0.216	Or 13	2,839	3.35	0.416	0.341
Gr 03	2,638	2.69	0.421	0.257	Or 13	2,839	3.35	0.389	0.402
Gr 03	2,638	2.69	0.387	0.296	Or 14	2,616	2.91	0.397	0.261
Gr 03	2,638	2.69	0.371	0.308	Or 14	2,616	2.91	0.293	0.392
Gr 04	2,603	2.66	0.442	0.242	Or 14	2,616	2.91	0.308	0.379
Gr 04	2,603	2.66	0.391	0.299	Or 14	2,616	2.91	0.413	0.246
Gr 04	2,603	2.66	0.361	0.325	Or 14	2,616	2.91	0.359	0.299
Gr 05	2,578	2.85	0.407	0.279	Or 14	2,616	2.91	0.338	0.329
Gr 05	2,578	2.85	0.368	0.315	Me 15	2,583	2.19	0.457	0.244
Gr 05	2,578	2.85	0.344	0.336	Me 15	2,583	2.19	0.402	0.303
Gr 06	2,593	3.00	0.447	0.239	Me 15	2,583	2.19	0.347	0.384
Gr 06	2,593	3.00	0.386	0.296	Me 16	2,632	2.29	0.562	0.182
Gr 06	2,593	3.00	0.350	0.361	Me 16	2,632	2.29	0.486	0.241
Gn 07	2,674	2.04	0.505	0.200	Me 16	2,632	2.29	0.459	0.270
Gn 07	2,674	2.04	0.451	0.243	Me 17	2,628	2.68	0.502	0.188
Gn 07	2,674	2.04	0.419	0.286	Me 17	2,628	2.68	0.433	0.238
Gn 08	2,830	2.05	0.489	0.249	Me 17	2,628	2.68	0.385	0.292
Gn 08	2,830	2.05	0.450	0.309	Me 18	2,569	3.50	0.436	0.244
Gn 08	2,830	2.05	0.400	0.346	Me 18	2,569	3.50	0.375	0.305
Gn 09	2,666	2.60	0.438	0.239	Me 18	2,569	3.50	0.353	0.328
Gn 09	2,666	2.60	0.369	0.302	Me 19	2,649	2.28	0.372	0.357
Gn 09	2,666	2.60	0.322	0.360	Me 19	2,649	2.28	0.467	0.236
Gn 10	2,647	2.54	0.446	0.244	Me 19	2,649	2.28	0.415	0.289
Gn 10	2,647	2.54	0.370	0.334	Me 19	2,649	2.28	0.388	0.338

range of the analyzed mixtures. In addition, the Geoterm model assumes that the mixture of interest consists of air-saturated, homogeneous and isotropic grains, the mixture phases are randomly distributed and the samples plot are within the external porosity region.

The points in Figure 2 represent measurements of samples at different porosities. To resolve the problem of predicting the thermal conductivity of the whole sample using the ETC and porosity measurements, we adjusted the Geoterm and Korvin models curves, independently, to the measurements of ETC of a same sample.

Figure 3 shows lines drawn between the limits of the Geoterm model that were obtained by varying the factor p in Eq. (13) from 0 to 1 in increments of 0.1, and Figure 4 shows lines drawn between the limits of the Korvin model that were obtained by varying t in Eq. (2) from −1 to 1.
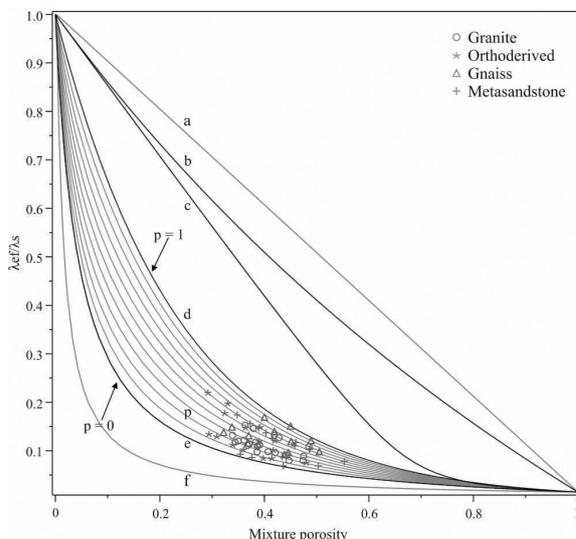
Figure 3 – Illustration of the curves in the region of the Geoterm model obtained by varying the weighting factor p from 0 to 1 in Eq. (13) in increments of 0.1.
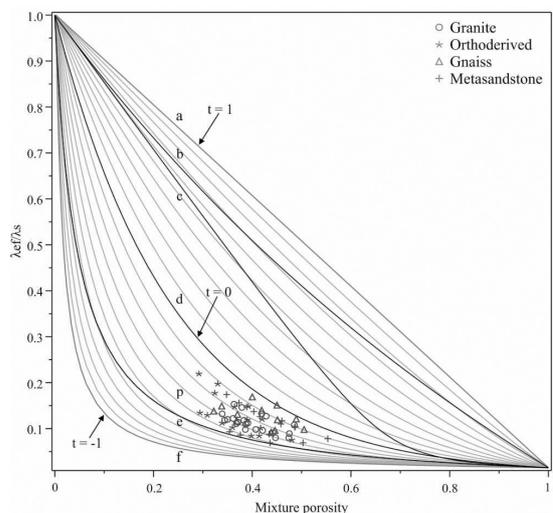

Figure 4 – Illustration of the curves in the region of the Korvin model obtained by varying the distribution factor t from –1 to 1 in Eq. (2) in increments of 0.1.

To use the Geoterm and Korvin models in the prediction problem (to obtain λ_s), we need to choose values for the factors p and t in Eqs. (13) and (2), respectively. We opted to use the average values of p and t that fit the curves of the Eqs. (13) and (2), respectively, in a graph of $\lambda_{ef} \times \phi$ to reproduce $\lambda_{ef} = \lambda_s$ at $\phi = 0$, taking the air thermal conductivity (λ_a) as 0.026 W m^{-1} K^{-1} at $\phi = 1$.

The adjustment process is exemplified in Figures 5 and 6. In sample Or 12 (Fig. 5), $\lambda_s = 2.01$ W m^{-1} k^{-1} and the curves of the Geoterm and Korvin models are fitted for $\lambda_{ef} = \lambda_s$ in the Eqs. (13) and (2) with $p = 0.576$ and $t = -0.142$, respectively. For sample Me 17 (Fig. 6) with $\lambda_s = 2.68$ W m^{-1} k^{-1}, $p = 0.505$ and $t = -0.160$.

As seen in Figure 5, all of the adjusted curves fit the experimental points of the samples well, which indicates that both the Geoterm and Korvin models are good heat conduction models for these mixtures for the porosity range used in this study.

Table 2 presents the factors p and t that reproduce the thermal conductivity λ_s of the whole rock for the Geoterm and Korvin models, respectively. The error associated to p and t is about of 10%. The ranges of variation of p and t are large: p varies from 0.386 to 1.037 with an average of 0.61 and a relative deviation of 28%, while t varies from –0.225 to 0.015 with an average of –0.13 and a relative deviation of 48%. These variations reflect the broad spectrum of thermal conductivity values for the different lithotypes and for the same type of rock, as has been reported by several authors (e.g., Clauser & Huenges, 1995; Labani & Anurup, 2007). All of these studies concluded that a given lithotype cannot be characterized by a single thermal conductivity value.

Figure 7 shows the curves of Eq. (13) for $p = 0.61$ and of Eq. (2) for $t = -0.13$ superimposed on the experimental data shown in Figure 2. These curves overlap in the porosity range of our measurements showing that both models are valid.

Using these average values to p and t, the λ_s and ϕ values from Table 1 and taking the air thermal conductivity as 0.026 W m^{-1} K^{-1}, we predict the ETC values using Eq. (13) for $p = 0.61$ and Eq. (2) for $t = -0.13$.

In Table 3, using data from Table 1, we show the measured ETC (λ_{ef}) and the predicted ETC (λ_{efp}) from the inferior Maxwell-Eucken (Eq. (6)), Geometric (Eq. (5)), Geoterm (Eq. (13)) and Korvin (Eq. (2)) models as well as from the Krupiczka (Eq. (10)) and Woodside-Messmer (Eq. (11)) expressions, together with the corresponding differences from the measured values.

Table 3 shows that the smallest differences are associated with the Geoterm and Korvin models and with the Woodside-Messmer empirical expression. This indicates that these models and expression can efficiently measure the ETC of air-saturated binary mixtures of rock grains.

To calculate the predicted thermal conductivity (λ_{sp}) of the whole rock, we make the adjustment shown in Figure 6 but now fixing p as 0.61 and t as –0.13 to obtain $\lambda_{sp} = \lambda_{ef}$ for $\phi = 0$. The calculating process is exemplified in Figures 8 and 9. The sample Me 17 (Fig. 8) has $\lambda_s = 2.68$ W m^{-1} K^{-1} and $\lambda_{sp} = 2.18$ W m^{-1} K^{-1} for the Geoterm model and $\lambda_{sp} = 2.48$ W m^{-1} K^{-1} for the Korvin model. For the sample Gr 01 (Fig. 9) with $\lambda_s = 2.11$ W m^{-1} K^{-1}, $\lambda_{sp} = 2.40$ W m^{-1} K^{-1} for the Geoterm model and $\lambda_{sp} = 2.41$ W m^{-1} K^{-1} for the Korvin model.
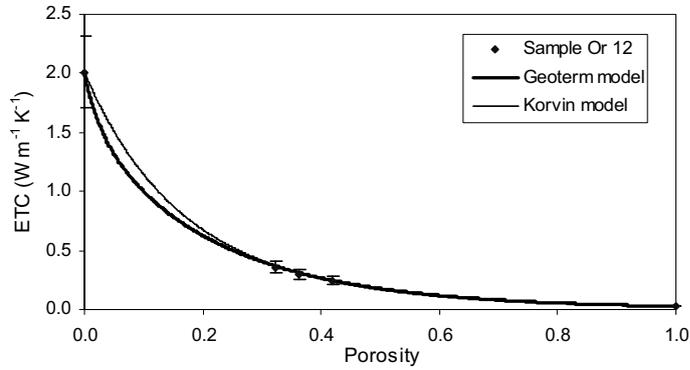
Figure 5 – Obtaining the factors p of the Geoterm model and t of the Korvin model by adjusting the curves of these models to the experimental data of sample Or 12 and to the points $\lambda_{ef} = \lambda_s$ at $\phi = 0$ and $\lambda_{ef} = \lambda_a$ at $\phi = 1$.

Figure 6 – Obtaining the factors p of the Geoterm model and t of the Korvin model by adjusting the curves of these models to the experimental data of sample Me 17 and to the points $\lambda_{ef} = \lambda_s$ at $\phi = 0$ and $\lambda_{ef} = \lambda_a$ at $\phi = 1$.
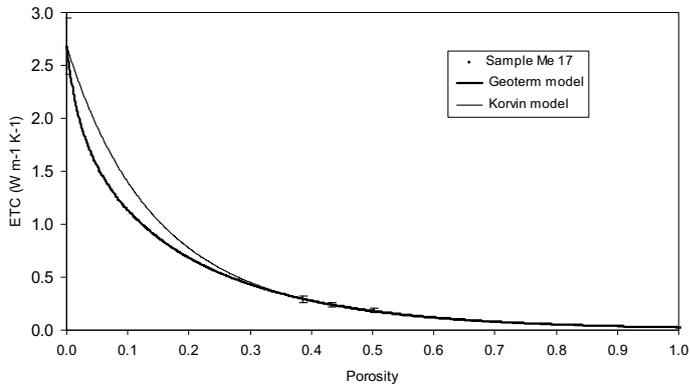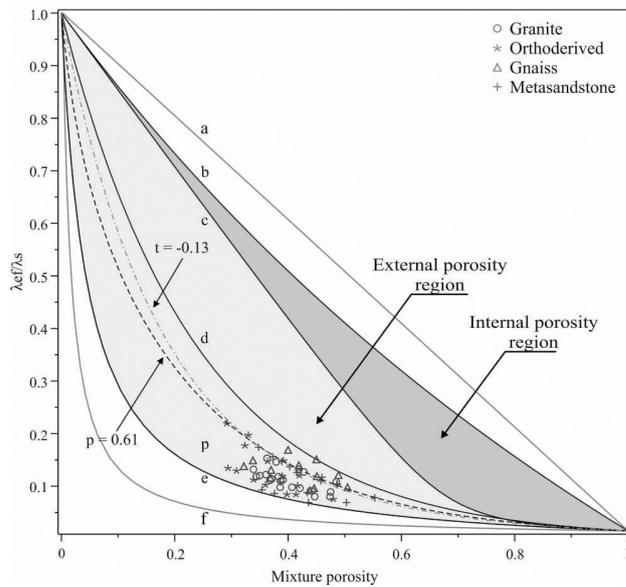

Figure 7 – Curves for $p = 0.61$ from Eq. (13) and $t = -0.13$ from Eq. (2) for the Geoterm and Korvin models, respectively, superimposed on the data shown in Figure 2.

Table 2 – Factors p and t that reproduce the real thermal conductivity in Eqs. (13) and (2), respectively.

Sample	Real value	Geoterm model	Korvin model
	λ_s, W m^{-1} k^{-1}	p	t
Gr 01	2.11	0.689	−0.095
Gr 02	2.20	0.457	−0.180
Gr 03	2.69	0.515	−0.155
Gr 04	2.66	0.526	−0.150
Gr 05	2.85	0.464	−0.180
Gr 06	3.00	0.481	−0.170
Gn 07	2.04	0.783	−0.060
Gn 08	2.05	1.037	+0.015
Gn 09	2.60	0.477	−0.172
Gn 10	2.54	0.593	−0.135
Or 11	1.75	0.626	−0.128
Or 12	2.01	0.576	−0.142
Or 13	3.35	0.687	−0.100
Or 14	2.91	0.386	−0.225
Me 15	2.19	0.730	−0.080
Me 16	2.29	0.882	−0.040
Me 17	2.68	0.505	−0.160
Me 18	3.50	0.386	−0.214
Me 19	2.28	0.734	−0.078
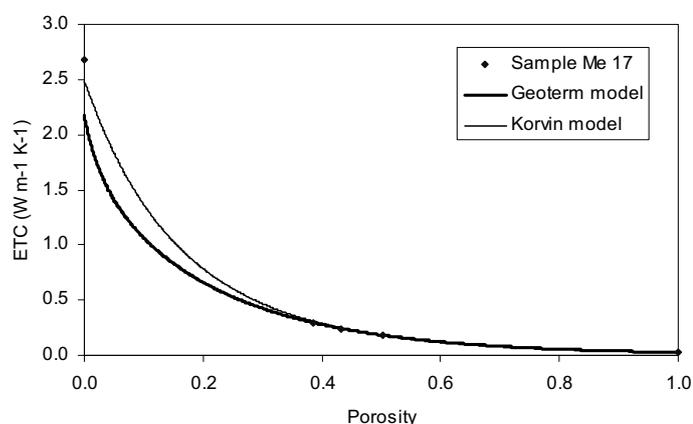
Figure 8 – Adjusting of the curves of the Geoterm model for $p = 0.61$ and Korvin model to $t = -0.13$ to the experimental data of the sample Me 17, and to the point $\lambda_{ef} = \lambda_a$ in $\phi = 1$, to obtain the predicted thermal conductivity $\lambda_{sp} = $ ETC in $\phi = 0$.

In Table 4 we present the predicted thermal conductivity of the whole rock obtained with the Geoterm and Korvin models making $p = 0.61$ and $t = -0.13$ in their respective equations and their respective discrepancies relative to the real λ_s.

The method developed in this work to obtain the rock thermal conductivity from binary granular mixtures proved effective. The large discrepancies observed in both models is because the

Eqs. (13) and (2) are quite sensitive to the values of p and t, respectively, so that values away from the reference values have discrepancies higher; and this not depend of the reference values, but of the width of the range variation of this factors. In the variation range of the porosity of the mixtures in this study, from 0.26 to 0.51, the curves of the Geoterm and Korvin models practically coincide only differing for porosities below about 0.25. Getting

Table 3 – Measured (λ_{ef}) and predicted (λ_{efp}) ETC values from the models and empirical expressions with the corresponding discrepancies relatives to the measured values. ETC values are in W m^{-1} K^{-1}.

| Sample | Measured | ME-I | | Geometric | | Geoterm | | Korvin | | Krupiczka | | Woodside | |
| | | Eq. (6) | | Eq. (5) | | Eq. (13) | | Eq. (2) | | Eq. (10) | | Eq. (11) | |
	λ_{ef}	λ_{efp}	δ, %	λ_{efp}	δ, %	λ_{efp}	δ, %	λ_{efp}	δ, %	λ_{efp}	δ, %	λ_{efp}	δ, %
Gr 01	0.228	0.108	52.0	0.271	19.0	0.198	13.0	0.203	0.2	0.166	27.0	0.237	3.8
Gr 01	0.268	0.122	54.0	0.321	20.0	0.232	13.0	0.241	10.0	0.188	30.0	0.265	1.1
Gr 01	0.278	0.125	55.0	0.334	20.0	0.240	14.0	0.251	10.0	0.194	30.0	0.271	2.4
Gr 01	0.308	0.142	54.0	0.399	29.0	0.283	8.0	0.301	2.3	0.224	27.0	0.302	2.0
Gr 01	0.323	0.150	54.0	0.428	32.0	0.303	6.3	0.324	0.3	0.239	26.0	0.314	2.7
Gr 02	0.195	0.106	46.0	0.267	37.0	0.195	0.1	0.199	2.1	0.164	16.0	0.233	19.0
Gr 02	0.259	0.141	46.0	0.402	55.0	0.284	9.8	0.301	16.0	0.224	13.0	0.301	16.0
Gr 02	0.291	0.164	44.0	0.489	68.0	0.342	18.0	0.370	27.0	0.268	8.0	0.336	16.0
Gr 03	0.216	0.108	50.0	0.298	38.0	0.212	1.6	0.216	0.2	0.175	19.0	0.241	11.0
Gr 03	0.257	0.126	51.0	0.382	48.0	0.267	3.8	0.277	7.8	0.209	19.0	0.281	9.4
Gr 03	0.296	0.141	52.0	0.447	51.0	0.309	4.4	0.326	10.0	0.238	20.0	0.309	4.2
Gr 03	0.308	0.149	52.0	0.481	56.0	0.331	7.6	0.352	14.0	0.254	18.0	0.322	4.5
Gr 04	0.242	0.118	51.0	0.344	42.0	0.242	0.2	0.250	3.2	0.194	20.0	0.264	9.2
Gr 04	0.299	0.139	54.0	0.436	46.0	0.302	1.0	0.318	6.3	0.233	22.0	0.305	1.9
Gr 04	0.325	0.154	53.0	0.500	54.0	0.344	5.9	0.368	13.0	0.264	19.0	0.330	1.4
Gr 05	0.279	0.132	53.0	0.421	51.0	0.291	4.4	0.304	8.9	0.225	19.0	0.295	5.7
Gr 05	0.315	0.151	52.0	0.506	61.0	0.346	9.9	0.368	17.0	0.263	17.0	0.327	3.9
Gr 05	0.336	0.164	51.0	0.566	69.0	0.385	15.0	0.414	23.0	0.292	13.0	0.348	3.6
Gr 06	0.239	0.117	51.0	0.359	50.0	0.250	4.7	0.257	7.3	0.198	17.0	0.265	11.0
Gr 06	0.296	0.142	52.0	0.480	63.0	0.328	11.0	0.345	17.0	0.249	16.0	0.315	6.6
Gr 06	0.361	0.161	55.0	0.569	58.0	0.385	6.8	0.413	14.0	0.290	20.0	0.346	4.2
Gn 07	0.200	0.097	51.0	0.225	13.0	0.168	16.0	0.170	15.0	0.147	27.0	0.210	4.9
Gn 07	0.243	0.113	53.0	0.285	17.0	0.208	14.0	0.215	12.0	0.173	29.0	0.247	1.5
Gn 07	0.286	0.125	56.0	0.328	15.0	0.237	17.0	0.247	14.0	0.192	33.0	0.270	5.7
Gn 08	0.249	0.102	59.0	0.242	2.7	0.179	28.0	0.182	27.0	0.154	38.0	0.221	11.0
Gn 08	0.309	0.114	63.0	0.287	7.1	0.209	32.0	0.216	30.0	0.173	44.0	0.247	20.0
Gn 08	0.346	0.133	62.0	0.357	3.3	0.256	26.0	0.270	22.0	0.205	41.0	0.284	18.0
Gn 09	0.239	0.120	50.0	0.346	45.0	0.244	2.1	0.252	5.5	0.195	18.0	0.266	11.0
Gn 09	0.302	0.149	51.0	0.475	57.0	0.329	8.8	0.350	16.0	0.253	16.0	0.322	6.5
Gn 09	0.360	0.176	51.0	0.590	64.0	0.404	12.0	0.440	22.0	0.311	14.0	0.362	0.5
Gn 10	0.244	0.117	52.0	0.329	35.0	0.233	4.3	0.241	1.4	0.188	23.0	0.259	6.3
Gn 10	0.334	0.149	56.0	0.466	40.0	0.323	3.2	0.344	3.0	0.249	25.0	0.320	4.3
Gn 10	0.378	0.166	56.0	0.540	43.0	0.372	1.7	0.402	6.2	0.286	24.0	0.347	8.3
Or 11	0.260	0.135	48.0	0.337	30.0	0.246	5.3	0.260	0.1	0.200	23.0	0.281	8.2
Or 11	0.346	0.166	52.0	0.438	27.0	0.316	8.8	0.342	1.0	0.254	27.0	0.327	5.4
Or 11	0.385	0.190	51.0	0.514	34.0	0.368	4.3	0.407	5.7	0.301	22.0	0.357	7.2
Or 12	0.243	0.125	49.0	0.325	34.0	0.235	3.3	0.246	1.0	0.191	21.0	0.269	11.0
Or 12	0.298	0.150	50.0	0.415	39.0	0.295	0.9	0.316	6.0	0.234	21.0	0.311	4.4
Or 12	0.358	0.172	52.0	0.494	38.0	0.349	2.6	0.380	6.2	0.277	23.0	0.343	4.2
Or 13	0.255	0.107	58.0	0.327	28.0	0.228	11.0	0.230	10.0	0.183	28.0	0.244	4.5
Or 13	0.341	0.130	62.0	0.444	30.0	0.302	11.0	0.313	8.3	0.229	33.0	0.294	14.0
Or 13	0.402	0.142	65.0	0.506	26.0	0.342	15.0	0.358	11.0	0.255	36.0	0.317	21.0

(to be continued)

Table 3 – (continuation)

| Sample	Measured	ME-I Eq. (6)		Geometric Eq. (5)		Geoterm Eq. (13)		Korvin Eq. (2)		Krupiczka Eq. (10)		Woodside Eq. (11)	
	λ_{ef}	λ_{efp}	δ, %	λ_{efp}	δ, %	λ_{efp}	δ, %	λ_{efp}	δ, %	λ_{efp}	δ, %	λ_{efp}	δ, %
Or 14	0.261	0.137	48.0	0.447	71.0	0.308	18.0	0.322	23.0	0.235	10.0	0.304	16.0
Or 14	0.392	0.198	49.0	0.730	86.0	0.491	25.0	0.543	39.0	0.377	4.0	0.396	0.9
Or 14	0.379	0.187	51.0	0.680	80.0	0.458	21.0	0.503	33.0	0.349	8.0	0.382	0.7
Or 14	0.246	0.130	47.0	0.415	69.0	0.287	16.0	0.298	21.0	0.221	10.0	0.291	18.0
Or 14	0.299	0.156	48.0	0.535	79.0	0.364	22.0	0.388	30.0	0.275	8.0	0.336	12.0
Or 14	0.329	0.167	49.0	0.591	80.0	0.400	22.0	0.432	31.0	0.302	8.2	0.355	7.8
Me 15	0.244	0.112	54.0	0.289	18.0	0.209	14.0	0.215	12.0	0.173	29.0	0.245	0.5
Me 15	0.303	0.132	56.0	0.368	22.0	0.262	13.0	0.276	9.0	0.209	31.0	0.286	5.6
Me 15	0.384	0.159	59.0	0.470	22.0	0.330	14.0	0.356	7.4	0.259	33.0	0.330	14.0
Me 16	0.182	0.086	53.0	0.193	6.2	0.145	20.0	0.145	20.0	0.133	27.0	0.183	0.5
Me 16	0.241	0.103	57.0	0.260	7.8	0.189	21.0	0.193	20.0	0.160	33.0	0.227	6.0
Me 16	0.270	0.112	59.0	0.293	8.6	0.211	22.0	0.217	20.0	0.175	35.0	0.246	9.0
Me 17	0.188	0.099	47.0	0.262	39.0	0.188	0.2	0.190	1.2	0.160	15.0	0.220	17.0
Me 17	0.238	0.122	49.0	0.360	51.0	0.253	6.2	0.261	10.0	0.200	16.0	0.272	14.0
Me 17	0.292	0.142	51.0	0.450	54.0	0.311	6.6	0.328	12.0	0.240	18.0	0.310	6.2
Me 18	0.244	0.122	50.0	0.415	70.0	0.283	16.0	0.290	19.0	0.217	11.0	0.280	15.0
Me 18	0.305	0.149	51.0	0.557	83.0	0.373	22.0	0.392	29.0	0.275	10.0	0.331	8.5
Me 18	0.328	0.160	51.0	0.620	89.0	0.413	26.0	0.440	34.0	0.303	7.6	0.351	6.9
Me 19	0.357	0.146	59.0	0.432	21.0	0.303	15.0	0.323	10.0	0.237	33.0	0.312	13.0
Me 19	0.236	0.109	54.0	0.282	20.0	0.204	13.0	0.209	11.0	0.170	28.0	0.240	1.6
Me 19	0.289	0.127	56.0	0.356	23.0	0.253	12.0	0.265	8.4	0.202	30.0	0.278	3.7
Me 19	0.338	0.139	59.0	0.402	19.0	0.284	16.0	0.300	11.0	0.223	34.0	0.299	12.0
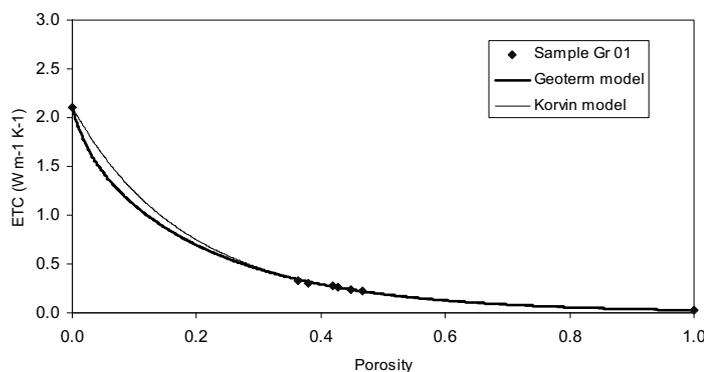
Figure 9 – Adjusting of the curves of the Geoterm model for $p = 0.61$ and Korvin model to $t = -0.13$ to the experimental data of the sample Gr 01, and to the point $\lambda_{ef} = \lambda_a$ in $\phi = 1$, to obtain the predicted thermal conductivity $\lambda_{sp} = \text{ETC}$ in $\phi = 0$.

mixtures with porosity below this value is difficult resulting in not have been possible to distinguish between these two models.

These variation ranges of p and t are larges because the thermal conductivity of rock is highly variable. The variability range of thermal conductivity is similar to all analyzed sam-ples and within each lithology. The question is to set up ranges narrower to p and t. The next step in this research is, therefore, seek semi-empirical expressions which include the characteris-tics of the mixtures as well as physical and geological character-istics of the rock.

Table 4 – Predicted thermal conductivity of the rock fully calculated with the models Geoterm for $p = 0.61$ and Korvin for $t = -0.13$ as well as their discrepancies respect of λ_s.

Sample	Real value	For $p = 0.61$		For $t = -0.13$	
	λ_s	λ_{sp}	δ, %	λ_{sp}	δ, %
Gr 01	2.11	2.40	14.0	2.41	14.0
Gr 02	2.20	1.66	25.0	1.70	23.0
Gr 03	2.69	2.20	18.0	2.30	14.0
Gr 04	2.66	2.25	15.0	2.40	10.0
Gr 05	2.85	2.14	25.0	2.20	23.0
Gr 06	3.00	2.32	23.0	2.36	21.0
Gn 07	2.04	2.70	32.0	2.90	42.0
Gn 08	2.05	3.83	87.0	4.30	110.0
Gn 09	2.60	2.03	22.0	2.00	23.0
Gn 10	2.54	2.42	4.7	2.58	1.5
Or 11	1.75	1.79	2.3	1.77	1.1
Or 12	2.01	1.90	5.5	1.90	5.5
Or 13	3.35	3.88	16.0	4.20	25.0
Or 14	2.91	1.85	36.0	1.80	38.0
Me 15	2.19	2.66	21.0	2.75	26.0
Me 16	2.29	3.63	59.0	4.30	88.0
Me 17	2.68	2.18	19.0	2.48	7.5
Me 18	3.50	2.14	39.0	2.12	39.0
Me 19	2.28	2.79	22.0	3.10	36.0

CONCLUSIONS

The Geoterm and Korvin heat conduction models showed to be effective in dealing with binary mixtures of rock grains air-saturated because their curves adjusted well to the experimental data of ETT. Moreover, both models showed good results in predicting the ETC measurements in the studied mixtures. Thus, the model and method developed in this work to determine the thermal conductivity of rock from ETC measurements in biphasic granular mixtures was showed to be effective.

The predicted results for the full sample, compared to the measured values, showed discrepancies small and large, a consequence of the range of variation of the thermal conductivity of the rocks to be well large resulting in ranges also large for the numerical factors of the two equations.

The Geoterm and Korvin heat conduction models proved to be effective in dealing with air-saturated binary mixtures of rock grains provided that their curves are adjusted based on ETC measurements. Moreover, both models showed good results in predicting the ETC measurements in the studied mixtures. Thus, the method developed in this work to determine the rock thermal conductivity from ETC measurements in binary granular mixtures was found to be effective.

When compared with the measured thermal conductivity of the solid rock, however, these results are not satisfactory. The p and t factors are highly variable, and the equations of the two models are quite sensitive to variations in these factors. We suggest defining narrower ranges of thermal conductivity values using data from granulated rock samples or drill cuttings.

REFERENCES

ANAND J, SOMERTON WH & GOMAA E. 1973. Predicting thermal conductivities of formations from other known properties. Society of Petroleum Engineers Journal, 13: 267–273.

CARSON JK, LOVATT SJ, TANNER DJ & CLELAND AC. 2005. Thermal conductivity bounds for isotropic, porous materials. International Journal of Heat and Mass Transfer, 48(11): 2150–2158.

CARSON JK, LOVATT SJ, TANNER DJ & CLELAND AC. 2006. Predicting the effective thermal conductivity of unfrozen, porous foods. Journal of Food Engineering, 75: 297–307.

CLAUSER C & HUENGES E. 1995. Thermal conductivity of rocks and minerals. In: AHRENS TJ (Ed.). Rock Physics & Phase Relations: A Handbook of Physical Constants. Washington, DC, American Geophysical Union, Reference Shelf, 3: 105–126.

KORVIN G. 1982. Axiomatic characterization of the general mixture rule. Geoexploration, 19: 267–276.

KRUPICZKA R. 1967. Analysis of thermal conductivity in granular materials. Int. Chem. Eng., 7: 122–144.

LABANI R & ANURUP B. 2007. Thermal conductivity of Higher Himalayan Crystallines from Garhwal Himalaya, Indian. Tectonophysics, 434: 71–79.

LANDAUER R. 1952. The electrical resistance of binary metallic mixtures. Journal of Applied Physics, 23: 779–784.

MAXWELL JC. 1954. Treatise on Electricity and Magnetism. 3rd ed., v.1, p. 2, Chapter 9, Dover, New York. 650 pp.

OLIVEIRA NB. 2006. Efeitos do gradiente do campo magnético na determinação da porosidade por ressonância magnética nuclear. Doctorate thesis, Universidade Federal da Bahia, Brazil, 114 pp. Available on: <http://www.pggeofisica.ufba.br/teses>. Access on: May 16, 2013.

TAVMAN IH. 1996. Effective thermal conductivity of granular porous materials. Int. Comm. Heat Mass Transfer, 23(2): 169–176.

TENCHOV GG. 1998. Evaluation of electrical conductivity of shaly sands using the theory of mixtures. Journal of Petroleum Science and Engineering, 21: 263–271.

WOODSIDE W & MESSMER JH. 1961. Thermal conductivity of porous media. Journal of Applied Physics, 32(9): 1688–1706.

NOTES ABOUT THE AUTHORS

Ariston de Lima Cardoso is BS in Physics from the Universidade Federal da Bahia (2003), MSc in Physics (2007) and PhD in Geophysics from the Universidade Federal da Bahia (2013). Currently, is an Adjunct Professor at the Center for Physical Sciences and Technology of the Universidade Federal do Recôncavo da Bahia. Current research interests involve thermal properties of rocks, blends systems and complex networks.

Roberto Max de Argollo is BS in Physics from the Universidade do Brasil (now UFRJ) (1963), MSc in Oceanography, University of Rhode Island, USA (1974) and PhD in Geophysics from the Universidade Federal da Bahia (2001). Is a retired full professor of the Physics Institute of the Universidade Federal da Bahia where remains bound to the postgraduate degree in Geophysics and as researcher at the Center for Research in Geophysics and Geology both of the Universidade Federal da Bahia. Current research interests involve thermal properties of rocks, radiogenic heat production in rocks and thermal structure of the lithosphere.

Alexandre Barreto Costa is BS in Physics from the Universidade Federal da Bahia (1997), MSc and PhD in Geophysics from the Universidade Federal da Bahia (2001/2006). Currently, is an Assistant Professor at UFBA. Has experience in Nuclear Geophysics, acting on the following topics: gamma spectrometry of sediments and rocks; radioactivity in groundwater; 14-Carbon dating; stable isotopes applied to water, organic matter and coral; and elementary analysis. Interest in the determination of radiogenic heat of rocks using gamma spectrometry measurements and thermal properties of rocks.